

# Spin transition of iron in magnesiowüstite in the Earth's lower mantle

Jung-Fu Lin<sup>1,†</sup>, Viktor V. Struzhkin<sup>1</sup>, Steven D. Jacobsen<sup>1</sup>, Michael Y. Hu<sup>2</sup>, Paul Chow<sup>2</sup>, Jennifer Kung<sup>3</sup>, Haozhe Liu<sup>2</sup>, Ho-kwang Mao<sup>1</sup> & Russell J. Hemley<sup>1</sup>

Iron is the most abundant transition-metal element in the mantle and therefore plays an important role in the geochemistry and geodynamics of the Earth's interior<sup>1–11</sup>. Pressure-induced electronic spin transitions of iron occur in magnesiowüstite, silicate perovskite and post-perovskite<sup>1–4,8,10,11</sup>. Here we have studied the spin states of iron in magnesiowüstite and the isolated effects of the electronic transitions on the elasticity of magnesiowüstite with *in situ* X-ray emission spectroscopy and X-ray diffraction to pressures of the lowermost mantle. An observed high-spin to low-spin transition of iron in magnesiowüstite results in an abnormal compressional behaviour between the high-spin and the low-spin states. The high-pressure, low-spin state exhibits a much higher bulk modulus and bulk sound velocity than the low-pressure, high-spin state; the bulk modulus jumps by ~35 per cent and bulk sound velocity increases by ~15 per cent across the transition in (Mg<sub>0.83</sub>,Fe<sub>0.17</sub>)O. Although no significant density change is observed across the electronic transition, the jump in the sound velocities and the bulk modulus across the transition provides an additional explanation for the seismic wave heterogeneity in the lowermost mantle<sup>12–21</sup>. The transition also affects current interpretations of the geophysical and geochemical models using extrapolated or calculated thermal equation-of-state data without considering the effects of the electronic transition<sup>5,6,22,23</sup>.

The electronic spin transition of iron in magnesiowüstite and silicate perovskite in the Earth's lower mantle has been postulated to have major geophysical and geochemical consequences: causing a large density change, shifting the partitioning of iron between magnesiowüstite and perovskite, altering radiative thermal conductivity, and enhancing compositional layering in the lower mantle<sup>1–4,8,10,11</sup>. However, no significant displacement in iron partitioning between magnesiowüstite and perovskite has been observed experimentally<sup>5–7</sup>, and the effects of the electronic transition on the density and elasticity have not previously been measured. Seismic observations show heterogeneities in seismic-wave velocities in the Earth's lower mantle<sup>12–18</sup>, where compositional and thermal variation, partial melting, and a phase transition in perovskite have been used to explain the origin of the heterogeneity<sup>16–21</sup>. Assuming a relatively large volume change across the spin transition and neglecting the spin-pairing energy of ~4 eV in thermodynamic calculations, it has been suggested that the partition coefficient of iron between magnesiowüstite and perovskite increases by several orders of magnitude in the mid- to lower mantle<sup>8</sup>, although *in-situ* X-ray diffraction and quenched sample analyses have not demonstrated such a dramatic change under mid- to lower-mantle conditions<sup>5–7</sup>.

To understand the consequences of the electronic transition on the geophysical and geochemical processes of the Earth's interior, we

have studied the spin states of iron in magnesiowüstite and the effects of the electronic transitions on the elasticity of magnesiowüstite with *in situ* X-ray emission spectroscopy (XES) and X-ray diffraction under lower-mantle pressures.

The spin states of iron in magnesiowüstite with varying Fe-content were probed by XES in a diamond anvil cell (Fig. 1). XES is an established technique that provides direct information on the local magnetic properties of iron atoms and has been widely used to study magnetic transitions in iron-containing systems<sup>8,10,11</sup>. The magnetic state of Fe is characterized by the appearance of the satellite emission peak ( $K\beta'$ ) located at the lower-energy region of the main emission

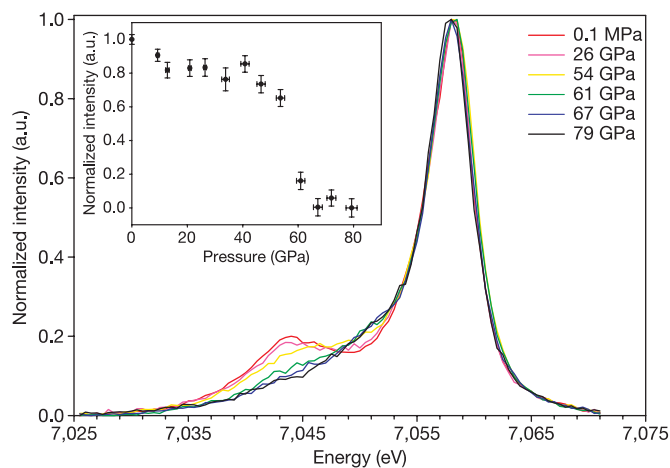


**Figure 1 | Representative X-ray emission spectra of Fe- $K\beta$  collected from a single-crystal magnesiowüstite, (Mg<sub>0.75</sub>,Fe<sub>0.25</sub>)O, in (110) orientation at high pressures.** The spectrum at ambient conditions was measured outside the diamond anvil cell. The spectra were normalized to unity and shifted in energy to compensate for the pressure-induced shift of the line maximum, based on the main fluorescence peak ( $K\beta$ ) at 7,058 eV. The presence of the satellite peak ( $K\beta'$ ) below 55 GPa is characteristic of the magnetic state of iron, whereas the absence of the satellite peak above 67 GPa indicates the collapse of the magnetization. Inset, normalized intensity of the satellite peak of iron in magnesiowüstite as a function of pressure. The intensity of the satellite peak was obtained by subtracting each spectrum from the one at the highest pressure (low-spin state). The errors in integrated intensity were propagated from statistical errors in original spectra (errors span two standard deviations). The intensity of the satellite peak is proportional to the magnetic moment of the iron atoms<sup>8,10,11</sup>, so the change in the intensity of the satellite peak can be used to understand the electronic spin transition of iron in magnesiowüstite. The observed electronic spin transition pressure for (Mg<sub>0.75</sub>,Fe<sub>0.25</sub>)O is close to the transition pressure in (Mg<sub>0.83</sub>,Fe<sub>0.17</sub>)O (ref. 8).

<sup>1</sup>Geophysical Laboratory, Carnegie Institution of Washington, 5251 Broad Branch Road NW, Washington DC 20015, USA. <sup>2</sup>HPCAT, Carnegie Institution of Washington, Advanced Photon Source, Argonne National Laboratory, Argonne, Illinois 60439, USA. <sup>3</sup>The Mineral Physics Institute, University of New York at Stony Brook, Stony Brook, New York 11794, USA. †Present address: Lawrence Livermore National Laboratory, 7000 East Avenue, Livermore, California 94550, USA.

peak ( $K\beta_{1,3}$ ) of  $\sim 7,058$  eV, which results from the  $3p-3d$  core-hole exchange interaction in the final state of the emission process. On the other hand, the collapse of the magnetization of Fe is characterized by the disappearance of the low-energy satellite owing to the loss of the  $3d$  magnetic moment. XES measurements of the Fe  $K\beta$  line were carried out at the High Pressure Collaborative Access Team (HPCAT) sector of the Advanced Photon Source (APS) at the Argonne National Laboratory. A monochromatic X-ray beam of 12 keV was focused down to  $20\ \mu\text{m}$  vertically and  $60\ \mu\text{m}$  horizontally at the sample position. The Fe  $K\beta$  emission spectra were collected through a Be gasket by an one-metre Rowland circle spectrometer in the vertical scattering geometry. A Si (333) single-crystal wafer glued onto a spherical substrate of one-metre radius was used as the analyser and a Peltier-cooled silicon detector (Amptek XR 100CR) was used to detect the emitted X-ray fluorescence. The sample was sandwiched between two layers of NaCl, and pressures were measured from rubies placed in the NaCl medium using the ruby pressure scale. The details of the experimental set-up<sup>8,10,11</sup> and sample syntheses<sup>24</sup> are reported elsewhere.

The XES spectra of the Fe  $K\beta$  fluorescence lines in  $(\text{Mg}_{0.75}\text{Fe}_{0.25})\text{O}$  and  $(\text{Mg}_{0.40}\text{Fe}_{0.60})\text{O}$  reveal that a high-spin to low-spin transition occurs at 54 to 67 GPa and 84 to 102 GPa, respectively (Fig. 1) (see

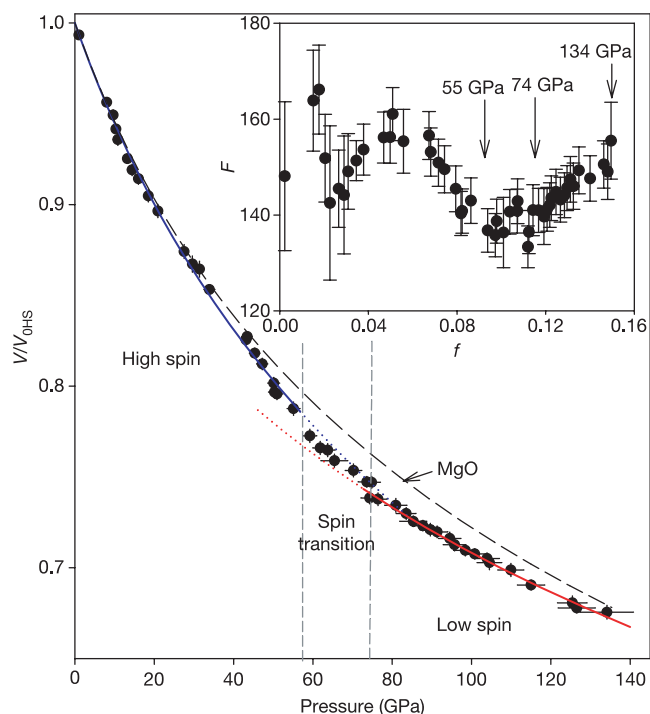


**Figure 2 | Normalized volume of magnesiowüstite,  $(\text{Mg}_{0.83}\text{Fe}_{0.17})\text{O}$ , as a function of pressure at 300 K.** A weighted least-squares fit to the high-spin state and low-spin state, based on the BM EOS (ref. 27), show that the  $K_{0T}$  and  $K_{0T}'$  of the high-spin state are  $160.7(\pm 3.7)$  and  $3.28(\pm 0.21)$  GPa (blue curve), respectively, whereas the  $K_{0T}$  of the low-spin state is  $250(\pm 28)$  GPa with a  $V_{0LS}/V_{0HS}$  of  $0.904(\pm 0.016)$  and an assumed  $K_{0T}'$  of 4 (red curve).  $V_{0HS}$  and  $V_{0LS}$  are the volumes of the high-spin state and low-spin state at ambient conditions, respectively. Based on the Vinet EOS (ref. 28), the  $K_{0T}$  and  $K_{0T}'$  of the high-spin state are  $161.3(\pm 5.2)$  and  $3.25(\pm 0.37)$  GPa, respectively, whereas the  $K_{0T}$  of the low-spin state is  $245(\pm 21)$  GPa, assuming a  $K_{0T}'$  of 4. The dashed black line represents the EOS of MgO with a  $K_{0T}$  of 160 GPa and  $K_{0T}'$  of 4 for comparison (ref. 25). The sample remains in the NaCl-type structure at all pressures<sup>9</sup>, and no significant change in density is observed. Inset, normalized stress ( $F$ ) versus normalized strain ( $f$ ) plot<sup>27</sup>.  $F$  decreases with increasing  $f$  up to 55 GPa, whereas  $F$  increases with increasing  $f$  above 74 GPa, indicating a significant change in the incompressibility from the high-spin state to the low-spin state. Error bars span two standard deviations.

Supplementary Information for details). To understand the isolated effect of the spin transition of iron on the elasticity of magnesiowüstite, we also carried out *in situ* X-ray powder diffraction experiments in a diamond anvil cell (Fig. 2). A polycrystalline magnesiowüstite sample—either  $(\text{Mg}_{0.83}\text{Fe}_{0.17})\text{O}$  or  $(\text{Mg}_{0.40}\text{Fe}_{0.60})\text{O}$ —was loaded into a diamond anvil cell with a neon pressure medium and Pt pressure scale<sup>25,26</sup>. The iron concentrations in  $(\text{Mg}_{0.75}\text{Fe}_{0.25})\text{O}$  and  $(\text{Mg}_{0.83}\text{Fe}_{0.17})\text{O}$  samples are close to the iron concentration in magnesiowüstite in the lower mantle, whereas the  $(\text{Mg}_{0.40}\text{Fe}_{0.60})\text{O}$  sample is used to understand the compositional effect on the spin transition and volume change. A focused monochromatic beam ( $0.4246\ \text{\AA}$ ) with a beam diameter of approximately  $10\ \mu\text{m}$  was used as the X-ray source for angle-dispersive X-ray diffraction experiments, and the diffracted X-ray was collected with an image plate (MAR345). Three diffraction peaks of (111), (200), and (220) were used to calculate the cell parameters of magnesiowüstite, and pressures were calculated from the equation of state (EOS) of Pt (refs 26, 27). Because the ruby pressure scale used during the XES studies was originally calibrated against the Pt pressure scale<sup>26</sup>, use of the Pt scale during X-ray diffraction measurements should yield precisely the same pressure as that obtained during the XES measurements. The pressure and volume data were analysed with the Birch–Murnaghan (BM) EOS and the Vinet EOS (refs 27, 28) using a weighted least-squares linear fit—the eulerian strain ( $f$ ) and the normalized stress ( $F$ ) in the BM EOS and  $\ln(H)$  and  $1 - X$  in the Vinet EOS—to obtain values for the isothermal bulk modulus ( $K_T$ ) at ambient conditions ( $K_{0T}$ ) and pressure derivative of the bulk modulus at ambient conditions ( $K_{0T}'$ ) (Fig. 2).

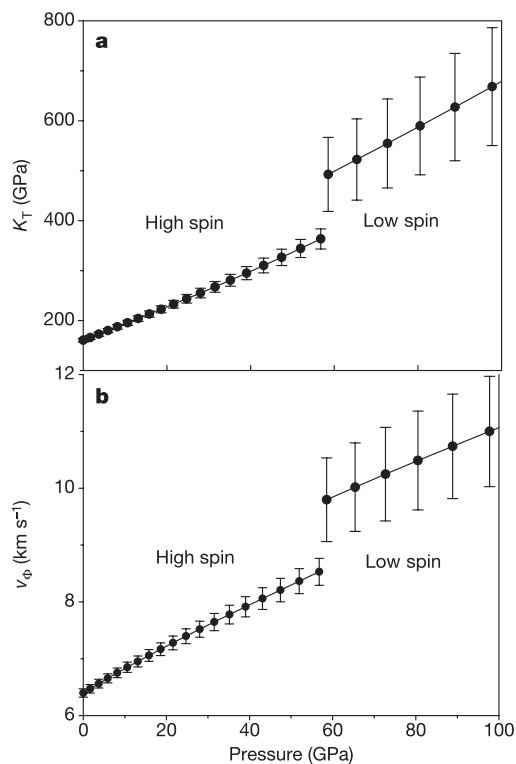


**Figure 3 | Calculated isothermal bulk modulus and bulk sound velocity as a function of pressure for the high-spin and low-spin states.** **a**, Bulk modulus; **b**, bulk sound velocity. Although no significant volume/density change was observed at approximately 60 GPa (ref. 8),  $K_T$  jumps by  $\sim 35\%$  across the transition. The bulk sound velocity ( $v_\Phi = \sqrt{K_S/\rho}$ ;  $K_S = K_T(1 + \alpha\gamma T)$ ;  $\alpha$  is the thermal expansion coefficient and  $\gamma$  is the Grüneisen parameter) increases by  $\sim 15\%$  across the transition. These values and their errors are calculated based on the BM EOS. These calculations based on the Vinet EOS show similar results. Error bars span two standard deviations.

Within experimental uncertainties, no significant volume or density change was observed in  $(\text{Mg}_{0.83}\text{Fe}_{0.17})\text{O}$  at approximately 60 GPa where the high-spin to low-spin transition has been observed by ref. 8 using XES (Figs 1, 2). On the other hand, a volume decrease of  $\sim 1.6\%$  was observed in  $(\text{Mg}_{0.40}\text{Fe}_{0.60})\text{O}$  at 95 GPa, consistent with the high-spin to low-spin transition pressure observed in XES studies. Our results show that addition of FeO in MgO stabilizes the high-spin state to higher pressures. The difference in effective ionic radii between octahedrally coordinated high-spin and low-spin  $\text{Fe}^{2+}$  in sulphides (based on the effective ionic radius of  $\text{O}^{2-}$  in six-fold coordination of 1.40 Å) is 0.16 Å, resulting in a volume change of 21% at ambient pressure<sup>29</sup>. It has been suggested that the electronic spin transition of Fe in iron-containing compounds can cause a significant volume reduction across the transition<sup>1,2,8,29</sup>. In  $\text{Fe}_2\text{O}_3$ , the volume change due to the electronic spin transition is estimated to be  $\sim 7\%$ ; however, a concurrent structure transition in  $\text{Fe}_2\text{O}_3$  complicates the estimation of the volume reduction<sup>30</sup>. It is believed that the composition of magnesiowüstite in the lower mantle<sup>5–7,22,23</sup> contains approximately 20% FeO, which corresponds to a density change of only  $\sim 0.5\%$  across the spin transition, according to our results. Considering that the lower mantle contains only approximately 20% of magnesiowüstite and that high temperature would further reduce the electronic effect on the density reduction, the very small density change is likely to be under the detection limit of current seismic-wave resolution.

By plotting the  $(\text{Mg,Fe})\text{O}$  compression data as normalized stress ( $F$ ) against eulerian strain ( $f$ ), it is possible to see the change in compressibility across the electronic transition (Fig. 2). These analyses show that the electronic transition significantly affects the incompressibility of magnesiowüstite at lower-mantle pressures. As shown, the normalized stress decreases with increasing the eulerian strain up to 55 GPa, whereas the normalized stress increases with increasing the eulerian strain above 74 GPa. We note that an electronic spin transition is observed in  $(\text{Mg}_{0.83}\text{Fe}_{0.17})\text{O}$  between 60 to 70 GPa (ref. 8). A weighted least-squares fit to the high-spin state and low-spin state, based on the BM EOS, shows that the  $K_{\text{OT}}$  and  $K_{\text{OT}'}$  of the high-spin state are  $160.7(\pm 3.7)$  and  $3.28(\pm 0.21)$  GPa, respectively, whereas the  $K_{\text{OT}}$  of the low-spin state is  $250(\pm 28)$  GPa with a  $V_{\text{OLS}}/V_{\text{OHS}}$  of  $0.904(\pm 0.016)$  and an assumed  $K_{\text{OT}'}$  of 4, where  $V_{\text{OHS}}$  and  $V_{\text{OLS}}$  are the volumes of the high-spin state and low-spin state at ambient conditions, respectively. These parameters remain similar on the basis of the Vinet EOS analyses (ref. 28), indicating that the incompressibility change does not depend on the form of the EOS used. The calculated  $K_{\text{T}}$  and bulk sound velocity ( $v_{\Phi} = \sqrt{(K_{\text{S}}/\rho)}$ , where  $K_{\text{S}}$  is the adiabatic bulk modulus and  $\rho$  is the density) show that a significant change in  $K_{\text{T}}$  and  $v_{\Phi}$  occurs across the transition and that the low-spin state has higher  $K_{\text{T}}$  and  $v_{\Phi}$  than the high-spin state (Fig. 3);  $K_{\text{T}}$  increases by  $\sim 35\%$  and  $v_{\Phi}$  increases by  $\sim 15\%$  across the transition.

The volume difference, change of entropy, and spin-pairing energy across the electronic transition are key parameters in estimating the thermodynamics of the spin transition, in particular Clapeyron slope and the partitioning of iron<sup>1,8,31,32</sup>. On the basis of our current XES and X-ray diffraction results (a small volume change) and thermodynamic considerations (the spin-pairing energy of 4.1 eV is considered in this study)<sup>31,32</sup>, we found that, for a magnesiowüstite containing  $\sim 20\%$  FeO, the Clapeyron slope of the high-spin to low-spin transition is approximately 56 K per GPa and the spin transition is shifted to  $\sim 120$  GPa at 2,500 K (close to the top of the  $D''$  region) (see Supplementary Information for details)<sup>32</sup>.

The unusual effects of the spin transition in iron on the elastic properties of magnesiowüstite reported here have several implications for the seismology, dynamics and geochemistry of the lower mantle. Recent seismic observations have shown that seismic wave heterogeneities exist in the Earth's lowermost mantle<sup>15,16,18</sup>; in particular, the shear-wave velocity ( $v_{\text{S}}$ ) changes more significantly than  $K_{\text{S}}$ ,  $v_{\text{P}}$  and  $v_{\Phi}$ . The changes in  $v_{\Phi}$  and  $v_{\text{S}}$  are anti-correlated<sup>12</sup>.

The phase transition from perovskite to post-perovskite has been used to explain the seismic-wave discontinuity in the  $D''$  layer<sup>19–21</sup>. Our results show that the electronic transition of iron in magnesiowüstite is likely to occur in the lowermost mantle and that the  $K_{\text{S}}$  and  $v_{\Phi}$  in magnesiowüstite would increase significantly across the transition in the lowermost mantle. Although the relatively less amount of magnesiowüstite in the lower mantle (approximately 20%) would reduce the magnitude of the effect on the elasticity, the electronic transition is still likely to leave a signature in the change of the sound velocities. Such a change in sound velocities provides an additional explanation for the seismic wave heterogeneities in the lowermost mantle<sup>15,16,18</sup>. The jump in  $v_{\Phi}$  across the electronic transition implies changes in  $v_{\text{P}}$  and  $v_{\text{S}}$ , so future ultrasonic or Brillouin studies on the  $v_{\text{P}}$  and  $v_{\text{S}}$  across the transition would provide crucial information in understanding the contribution of the electronic transition to this seismic-wave heterogeneity.

The electronic spin transition in iron has also been reported for both ferromagnesian silicate perovskite and the post-perovskite phase<sup>10</sup>. The electronic transitions should also affect the incompressibility and sound velocities in perovskite and post-perovskite. We also observed optically that the opacity of the magnesiowüstite increases with increasing pressure and the low-spin state can be well heated by the radiation of the Nd:YLF laser at 1,053 nm; the heated magnesiowüstite sample across the transition remains in the NaCl-type structure, as revealed from *in situ* X-ray diffraction. The enhanced opacity of  $(\text{Mg,Fe})\text{O}$  above the transition is at odds with that predicted theoretically<sup>2</sup>. One possible explanation is that in ref. 2 only the average energy of the excited singlet states of low-spin  $\text{Fe}^{2+}$  was estimated. Because the post-perovskite is suggested to be transparent in the infrared region, the low-spin state of magnesiowüstite may become dominant in blocking radiative heat transfer in the lowermost mantle.

Our current understanding of the EOS for iron-bearing minerals comprising the bulk of the Earth's lower mantle, namely magnesiowüstite and ferromagnesian silicate perovskite, appears to be inadequate, considering the effects of the pressure-induced spin-state transitions in Fe. We present experimental evidence for the anomalous compressibility of magnesiowüstite through the high-spin to low-spin transition, indicating that an extrapolation of the low-pressure, high-spin EOS inaccurately predicts the density of magnesiowüstite in deeper parts of the lower mantle. Furthermore, a discontinuous jump in the  $K_{\text{T}}$  and  $v_{\Phi}$  values measured in this study may account for the seismic-wave heterogeneities in the lowermost mantle. It remains to be seen how the spin-state transitions in the lower mantle will affect shear velocities of these phases, but the emerging picture of the Earth's deeper mantle from complementary seismic and mineral physics studies suggest that it is a more complex region than traditionally thought.

Received 17 January; accepted 13 May 2005.

1. Sherman, D. M. in *Structural and Magnetic Phase Transitions in Minerals* (eds Ghose, S., Coey, J. M. D. & Salje, E.) 113–118 (Springer, New York, 1988).
2. Sherman, D. M. The high-pressure electronic structure of magnesiowüstite  $(\text{Mg,Fe})\text{O}$ : applications to the physics and chemistry of the lower mantle. *J. Geophys. Res.* **96**(B9), 14299–14312 (1991).
3. Sherman, D. M. & Jansen, H. J. F. First-principles predictions of the high-pressure phase transition and electronic structure of FeO: implications for the chemistry of the lower mantle and core. *Geophys. Res. Lett.* **22**, 1001–1004 (1995).
4. Cohen, R. E., Mazin, I. I. & Isaak, D. G. Magnetic collapse in transition metal oxides at high pressure: implications for the Earth. *Science* **275**, 654–657 (1997).
5. Mao, H. K., Shen, G. & Hemley, R. J. Multivariable dependence of Fe-Mg partitioning in the lower mantle. *Science* **278**, 2098–2100 (1997).
6. Andraut, D. Evaluation of  $(\text{Mg,Fe})$  partitioning between silicate perovskite and magnesiowüstite up to 120 GPa and 2300 K. *J. Geophys. Res.* **106**, 2079–2087 (2001).
7. Kesson, S. E., Fitz Gerald, J. D., O'Neill, H., St. C. & Shelley, J. M. G. Partitioning of iron between magnesian silicate perovskite and magnesiowüstite at about 1 Mbar. *Phys. Earth Planet. Inter.* **131**, 295–310 (2002).

8. Badro, J. *et al.* Iron partitioning in Earth's mantle: toward a deep lower mantle discontinuity. *Science* **300**, 789–791 (2003).
9. Lin, J. F. *et al.* Stability of magnesiowüstite in the Earth's lower mantle. *Proc. Natl Acad. Sci. USA* **100**, 4405–4408 (2003).
10. Badro, J. *et al.* Electronic transitions in perovskite: possible nonconvecting layers in the lower mantle. *Science* **305**, 383–386 (2004).
11. Li, J. *et al.* Electronic spin state of iron in lower mantle perovskite. *Proc. Natl Acad. Sci. USA* **101**, 14027–14030 (2004).
12. Su, W. J. & Dziewonski, A. M. Simultaneous inversion for 3-D variations in shear and bulk velocity in the mantle. *Phys. Earth Planet. Inter.* **100**, 135–156 (1997).
13. Kellogg, L. H., Hager, B. H. & van der Hilst, R. D. Compositional stratification in the deep mantle. *Science* **283**, 1881–1884 (1999).
14. van der Hilst, R. D. & Kárason, H. Compositional heterogeneity in the bottom 1000 kilometers of Earth's mantle: toward a hybrid convection model. *Science* **283**, 1885–1888 (1999).
15. Garnero, E. Heterogeneity of the lowermost mantle. *Annu. Rev. Earth Planet. Sci.* **28**, 509–537 (2000).
16. Masters, G., Laske, G., Bolton, H. & Dziewonski, A. M. in *Earth's Deep Interior: Mineral Physics and Tomography From the Atomic to the Global Scale* (eds Karato, S., Forte, A. M., Liebermann, R. C., Masters, G. & Stixrude, L.) 63–87 (American Geophysical Union, Washington DC, 2000).
17. Karato, S. I. & Kaiki, B. B. Origin of lateral variation of seismic wave velocities and density in the deep mantle. *J. Geophys. Res.* **106**, 21771–21783 (2001).
18. Lay, T., Garnero, E. J. & Williams, Q. Partial melting in a thermo-chemical boundary layer at the base of the mantle. *Phys. Earth Planet. Inter.* **146**, 441–467 (2004).
19. Murakami, M., Hirose, K., Kawamura, K., Sata, N. & Ohishi, Y. Post-perovskite phase transition in MgSiO<sub>3</sub>. *Science* **304**, 855–858 (2004).
20. Oganov, A. R. & Ono, S. Theoretical and experimental evidence for a post-perovskite phase of MgSiO<sub>3</sub> in Earth's D'' layer. *Nature* **430**, 445–448 (2004).
21. Tsuchiya, T., Tsuchiya, J., Umemoto, K. & Wentzcovitch, R. M. Elasticity of post-perovskite MgSiO<sub>3</sub>. *Geophys. Res. Lett.* **31**, L14603, doi:10.1029/2004GL020278 (2004).
22. Jackson, I. Elasticity, composition and temperature of the Earth's lower mantle: a reappraisal. *Geophys. J. Int.* **134**, 291–311 (1998).
23. Stacey, F. D. & Isaak, D. G. Compositional constraints on the equation of state and thermal properties of the lower mantle. *Geophys. J. Int.* **146**, 143–154 (2001).
24. Jacobsen, S. D. *et al.* Structure and elasticity of single-crystal (Mg,Fe)O and a new method of generating shear waves for gigahertz ultrasonic interferometry. *J. Geophys. Res.* **107**(B2), 10.1029/2001JB000490 (2002).
25. Speziale, S., Zha, C. S., Duffy, T. S., Hemley, R. J. & Mao, H. K. Quasi-hydrostatic compression of magnesium oxide to 52 GPa: Implications for the pressure-volume-temperature equation of state. *J. Geophys. Res.* **106**, 515–528 (2001).
26. Holmes, N. C., Moriarty, J. A., Gathers, G. R. & Nellis, W. J. The equation of state of platinum to 660 GPa (6.6 Mbar). *J. Appl. Phys.* **66**, 2962–2967 (1989).
27. Birch, F. Equation of state and thermodynamic parameters of NaCl to 300 kbar in the high-temperature domain. *J. Geophys. Res.* **91**, 4949–4954 (1986).
28. Vinet, P., Ferrante, J., Rose, J. H. & Smith, J. R. Compressibility of solids. *J. Geophys. Res.* **92**, 9319–9325 (1987).
29. Shannon, R. D. & Prewitt, C. T. Effective ionic radii in oxides and fluorides. *Acta Crystallogr.* **B25**, 925–946 (1969).
30. Badro, J. *et al.* Nature of the high-pressure transition in Fe<sub>2</sub>O<sub>3</sub> hematite. *Phys. Rev. Lett.* **89**, 205504 (2002).
31. Burns, R. G. *Mineralogical Applications of Crystal Field Theory* Ch. 2, 7–43 (Cambridge Univ. Press, Cambridge, 1993).
32. Brown, J. M. & Shankland, T. J. Thermodynamic parameters in the Earth as determined from seismic profiles. *Geophys. J. R. Astron. Soc.* **66**, 579–596 (1981).

**Supplementary Information** is linked to the online version of the paper at [www.nature.com/nature](http://www.nature.com/nature).

**Acknowledgements** We thank R. Caracas, R. Cohen, G. Shen, V. Prakapenka, W. Sturhahn, J. M. Jackson, P. Silver, B. Militzer, S. Hardy, C. Prewitt, M. Somayazulu, P. Dera, and Y. Fei for discussions, S. J. Mackwell for help with sample synthesis, HPCAT for the use of the X-ray facilities, and GSECARS, APS, for the use of the Raman system. This work and use of the APS are supported by the US Department of Energy, Basic Energy Sciences, Office of Science and the State of Illinois under HECA. Work at Carnegie was supported by DOE/BES, DOE/NNSA (CDAC), NSF, and the W. M. Keck Foundation.

**Author Information** Reprints and permissions information is available at [npg.nature.com/reprintsandpermissions](http://npg.nature.com/reprintsandpermissions). The authors declare no competing financial interests. Correspondence and requests for materials should be addressed to J.-F.L. ([j.lin@gl.ciw.edu](mailto:j.lin@gl.ciw.edu)).